Poly(*p*-phenylene sulfide)/Liquid Crystalline Polymer Blends. II. Crystallization Kinetics

G. GABELLINI and R. E. S. BRETAS*

Department of Materials Engineering, Universidade Federal de Sao Carlos, 13565-905 Sao Carlos, SP, Brasil

SYNOPSIS

The crystallization kinetics of blends made of poly(p-phenylene sulfide) (PPS), with a liquid crystalline polymer (LCP) was studied. The blends were found to be immiscible by dynamic mechanical thermal analysis (DMTA). Results of non-isothermal and isothermal crystallization experiments made by differential scanning calorimetry (DSC) showed that both components had their crystallization temperatures increased; also the LCP melting temperature was found to increase in the blends. It was concluded that the addition of LCP to the PPS increased the PPS overall crystallization rate due to heterogeneous nucleation. The fold interfacial free energy, σ_e, of the PPS in the blends was observed not to vary with composition. © 1996 John Wiley & Sons, Inc.

INTRODUCTION

Poly(*p*-phenylene sulfide) (PPS) is a semicrystalline polymer that has been increasingly used as an engineering thermoplastic, mainly due to its high thermal and chemical resistance and mechanical strength. These outstanding properties can be attributed to its chemical structure, composed of phenyl groups linked by a sulfur atom, which gives rigidity to the chain, and also to its degree of crystallinity. This degree of crystallinity can be varied by using different thermal treatments, by changing its molecular weight, and by the addition of reinforcing inorganic fillers. All these factors affect the PPS overall crystallization rate.

This overall crystallization rate has been extensively studied. Lovinger et al.[1] found, e.g., that the transition for regime II to III is centered at 208°C; however, they did not observe a regime I to II transition. They also calculated the fold interfacial free energy, σ_e, using the Hoffmann and Lauritzen kinetics theory, without the reptation term.[2] The influence of molecular weight on the PPS crystallization kinetics was also studied; a recent work[3] confirmed that, as predicted by Hoffmann and Miller[4] using the reptation concept, the crystallization growth rate of this polymer is inversely proportional to its molecular weight. In another work,[5] in which the Ozawa analysis was applied, Avrami exponents, n, between 2 and 3 were found. Even the crystallization kinetics of PPS as a function of a branching agent content and the chemical nature of the end groups was also studied,[6] giving the Avrami exponent $n = 3$.

When PPS is blended with another polymer like poly(ethylene terephthalate) (PET),[7] it was observed that the nonisothermal crystallization of both components is modified; however, the extent of modification seems not to be significant for PPS. Another study[8] of this blend found that the nucleation of PPS, in a nonisothermal crystallization, is unaffected by the presence of the PET; however, in an isothermal crystallization, the PPS crystallization rate is found to be higher when blended with PET.

When inorganic fibers were added to PPS, it was observed that these fibers also affect the crystallization kinetics and the final amount of crystallinity[7,9]; the formation of PPS transcrystallites on the fiber surface was also observed.[9]

When a liquid crystalline polymer (LCP) is incorporated into the PPS matrix, the crystallization kinetics can also be affected. Depending on the mis-

* To whom correspondence should be addressed.

Journal of Applied Polymer Science, Vol. 61, 1803-1812 (1996)
 CCC 0021-8995/96/101803-10

cibility of both components, on the critical concentration, C^*, and on the deformational field (shear or extension), the LCP might form fibrils.[10,11] Therefore, the overall crystallization rate will also depend on these factors. Budgell and Day[12] studied the crystallization kinetics of blends of two kinds of PPS (Fortron and Ryton) with an LCP (Vectra A950, Hoechst) in the range of 10–50 wt % LCP. Fortron is a more linear PPS than is Ryton. They found that this particular LCP sligthly retards the Fortron PPS crystallization, but has little effect on the Ryton PPS, even not being miscible with both of them. However, calculation of σ_e was not reported. In this regard, we observed[13] that blends of poly(ether ether ketone) (PEEK) with an LCP (HX4000, DuPont), which present miscibility of its amorphous parts in the solid state, have the PEEK overall crystallization rate retarded due to the presence of the LCP molecules, and less perfect PEEK crystals and more perfect LCP domains are produced as a consequence. Also, we observed that both the lateral interfacial free energy, σ, and σ_e, are modified by the presence of the LCP. Another study[14] on the crystallization of blends of PPS with an LCP (Vectra, Hoechst) showed that, in this case, the nonisothermal crystallization temperature T_c and the equilibrium melting temperature, T_m^0, of the PPS are not affected by the concentration of the LCP and that this last polymer does not act as a nucleation agent for the PPS.

In the first part of this work,[15] the miscibility and morphology of PPS and its blends with an LCP (HX4000, DuPont) were studied. It was observed that the C^* for these blends was between 20–25 wt % LCP, that in the melt and solid states the LCP was immiscible with the PPS, and, finally, that the PPS formed transcrystallites on the surface of the LCP fibrils. Therefore, the LCP fibrils could act as nucleation agents for the PPS, promoting heterogeneous nucleation. As a consequence, the second part of this work will be related to the influence that this particular LCP has on the PPS overall crystallization kinetics.

EXPERIMENTAL

Materials

The PPS was from Phillips Petroleum Co. (Ryton V-1) and the LCP was from DuPont (HX4000). The blending was done as reported in Ref. 15.

Differential Scanning Calorimetry (DSC)

All the thermal experiments were performed in a differential scanning calorimeter DSC-7 (Perkin-Elmer) after routine calibration with In and Zn. The sample masses were between 10 and 11 mg. Each experiment was done twice and sometimes three times, under N2 atmosphere.

Nonisothermal Crystallization

The heating runnings were done at 5, 10, and 20°C/min on samples as received (injection-molded); the cooling runs were done at the same absolute rates, after melting at 350°C, for 5 min.

Isothermal Crystallization

To perform these experiments, the samples were heated at 20°C/min, melted at 350°C for 10 min, and then cooled down at −200°C/min up to the following crystallization temperatures, T_c: 240, 245, 247.5, and 250°C. It is known that PPS cures at approximately 300°C in the presence of air[16]; however, its equilibrium melting temperature is in the range of 301–357°C.[17] One report even showed that complete melting of PPS occurs between 330 and 350°C.[12] Also, a recent study[18] using thermogravimetric analysis (TGA) showed that pure PPS is stable up to 450°C. Therefore, we believed that, in order to destroy all remanescent crystallinity and avoid self-nucleation, a temperature of 350°C was suitable.

Equilibrium Melting Point

To determine T_m^0, the Hoffmann and Weeks approach was used,[2] where

$$T_m = T_m^0(1 - 1/\gamma) + T_c/\gamma$$

and γ = lamellar thickening factor (the final lamellar thickness will be γ times larger than the initial thickness). T_m^0 is the intercept of the extrapolated melting temperatures, T_m, and the straight line $T_m = T_c$. The blends were crystallized isothermally at different T_c's from the melt state, as said before; after crystallization was done, T_m was measured, at a heating rate of 20°C/min.

THEORETICAL BACKGROUND

The Avrami parameters, n and k, can be calculated from[19]:

$$\ln\{[1 - X_c(t)/X_\infty]\} = -kt^n \quad (1)$$

where $X_c(t)$ = degree of crystallinity as a function of time and X_∞ = ultimate crystallinity at very long times. The n parameter can often be related to the dimensionality of the morphology of the crystals and to the way primary nuclei are formed; the k parameter is proportional to the overall crystallization rate, G.[20,21]

G can be expressed, from the Hoffmann and Lauritzen theory,[2] without reptation, as

$$G = G_0 \exp[-U^*/R(T_c - T_\infty)] \times \exp[-rb_0\sigma\sigma_e/\Delta f K T_c] \quad (2)$$

where G_0 = preexponential factor (independent of temperature but depending on molecular weight and chain mobility); r = parameter characteristic of the crystallization growth regime (4 for regimes I and III and 2 for regime II); b_0 = thickness of the surface nucleus; $\Delta f = [\Delta H_m^0 \Delta T/T_m^0]f$; $f = 2\ T_c/(T_m^0 + T_c)$; ΔH_m^0 = equilibrium heat of fusion; and K = the Boltzmann constant.

From the Avrami approach, it follows that

$$k \propto G^n$$

Therefore, eq. (2) can be written as

$$\alpha = (\ln k)/n + U^*/R(T_c - T_\infty) = \ln G_0 - rb_0\sigma\sigma_e/(\Delta f)KT_c. \quad (3)$$

By plotting α as a function of $1/(\Delta f)T$ (or $1/T\Delta Tf$), σ_e can be calculated if the other parameters are known.

In a miscible blend, one of the components can be regarded as a diluent, and σ_e can also be calculated from the following expression[21,22]:

$$\alpha = (\ln k)/n + U^*/R[T_c - T_\infty(\phi)] - [1 + 2\sigma T_m^0(\phi)/b_0 f \Delta H_m^0 \Delta T(\phi)]\ln\phi = \ln G_0 - rb_0\sigma\sigma_e T_m^0(\phi)/Kf\Delta H_m^0 T\Delta T(\phi) \quad (4)$$

where ϕ = volume fraction of the crystallizable polymer.

U^* and $T_\infty = T_g - C_2$, where T_g is the glass transition temperature and C_2 is the WLF constant, can be taken from the WLF equation; but as pointed out,[1] these values are more associated with viscoelastic measurements than to crystallization rate analysis.

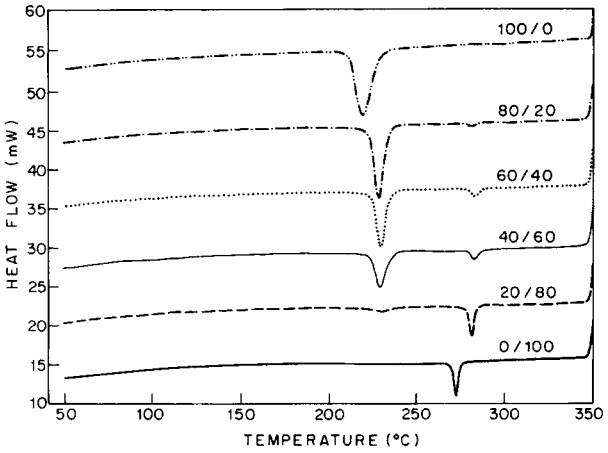

Figure 1 Nonisothermal crystallization experiments of the PPS/HX4000 blends, from the melt, at −10°C/min.

RESULTS AND DISCUSSION

Nonisothermal Crystallization

Figure 1 shows typical nonisothermal crystallization curves of the blends from the melt. Two crystallization peaks can be observed. The high-temperature peak ($T_{ccHX4000}$) corresponds to the HX4000 crystallization and the low-temperature one (T_{ccPPS}) corresponds to the PPS crystallization. There were always two peaks, independent of temperature. The PPS melt crystallized in the presence of already crystallized HX4000 domains. Both temperatures and the crystallization entalphies (ΔH_{cc}) of the blends as a function of the cooling rate are given in Table I.

It can be observed that, independent of the cooling rate, the nonisothermal crystallization of the PPS in the blends occurs at higher temperatures ($\sim$ 10°C) than does that of the pure polymer, indicating that the HX4000 accelerates this process. However, the PPS has the same influence on the HX4000 nonisothermal crystallization, increasing the HX4000 crystallization temperature also by $\sim$ 10°C. These results are in contrast with those reported by Budgell and Day[12]; they concluded that the LCP acted as a crystallization inhibitor. However, their premelting history (melt time and blending processes) and LCP chemical structure were different from ours. Their blends were extruded, while ours were injection-molded; they did not mention

the melt time at which the samples were held after melting in the DSC. Ours was 5 min. Therefore, we assume that our melt time was sufficient to allow complete phase separation of both components and, consequently, allows the LCP to act as a nucleation agent. Probably, their melt time was less than 5 min, not enough for phase separation to occur, because the PPS, being more disperse, would have its diffusion difficult and, consequently, crystallization would occur at a later time.

In our case, the increase of the PPS nonisothermal crystallization temperature can be attributed to the fact that already crystallized HX4000 domains are acting as nucleation agents for the PPS macromolecules.[15] The increase of the HX4000 nonisothermal crystallization temperature is more difficult to explain, but can be related to the way the LCPs crystallize. As pointed out by other authors,[23] crystallization of a pure LCP from the melt may take place in two steps: (a) cooperative ordering of the "rigid-rod"-like chains into a parallel alignment and (b) increase in intermolecular interactions due to the more efficient packing of the chains in the parallel state. When the HX4000 is blended with the PPS, in the melt, due to its immiscibility with this polymer, the HX4000 molecules will segregate into aggregates and, therefore, the formation of parallel domains (step a) will be easier than in the pure state. Step b will limit itself to the increase of the packing of the chains. The HX4000 overall crystallization rate will be controlled mainly by step a. Therefore, it will occur at a higher temperature than in the pure state.

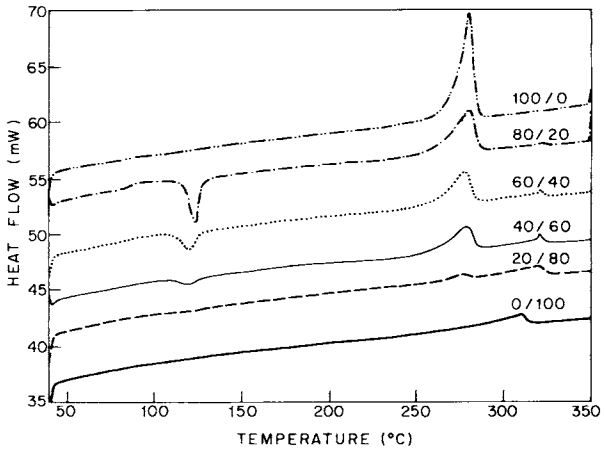

Figure 2 Typical heating scan of the PPS/HX4000 blends, at 10°C/min.

Figure 2 shows a typical heating scan of the blends. One cold crystallization and two melting peaks can be observed. The crystallization peak corresponds to the PPS, $T_{c\mathrm{PPS}}$; the lower melting endotherm, $T_{m\mathrm{PPS}}$, corresponds to the PPS; and the higher one corresponds to the HX4000, $T_{m\mathrm{HX4000}}$. The blends were prepared by injection molding, at an average temperature of 350°C; the mold temperature was set at 60°C.[15] The residence time at the

Table I Data of the Nonisothermal Crystallization of the PPS/HX4000 Blends

Cooling Rate	Blend PPS/HX4000	$T_{cc\mathrm{HX4000}}$ (°C)	ΔH_{cc} (HX4000) (J/g)	$T_{cc\mathrm{PPS}}$ (°C)	ΔH_{cc} (PPS) (J/g)
−5°C/min	100/0	—	—	226.1	52.48
	80/20	285.8	1.35	236.0	35.91
	60/40	284.4	2.97	236.0	27.10
	40/60	287.3	5.05	235.3	18.05
	20/80	284.3	8.32	237.7	2.74
	0/100	275.7	8.16	—	—
−10°C/min	100/0	—	—	281.8	51.36
	80/20	281.4	1.25	228.3	37.72
	60/40	282.5	3.47	229.5	28.54
	40/60	283.2	4.01	229.2	20.39
	20/80	281.2	8.31	230.5	3.13
	0/100	272.3	13.24	—	—
−20°C/min	100/0	—	—	210.9	50.55
	80/20	277.8	1.53	220.9	34.92
	60/40	278.8	2.50	222.7	28.93
	40/60	278.5	5.57	224.0	12.54
	20/80	278.1	7.58	223.4	3.42
	0/100	269.5	15.21	—	—

Table II Data of the Heating Experiments of the PPS/HX4000 Blends

Blend PPS/HX4000	T_{cPPS} (°C)	T_{mPPS} (°C)	ΔH_{mPPS} (J/g)	$T_{mHX4000}$ (°C)	$\Delta H_{mHX4000}$ (J/g)
Heating rate: 5°C/min					
100/0	—	282.6	50.04	—	—
80/20	119.9	279.5	31.57	322.6	0.61
60/40	119.2	279.8	20.09	321.6	1.81
40/60	118.7	279.9	14.79	323.9	5.12
20/80	117.4	279.1	4.15	322.0	7.27
0/100	—	—	—	311.3	6.83
Heating rate: 10°C/min					
100/0	—	281.5	56.76	—	—
80/20	124.0	280.9	33.18	323.0	0.94
60/40	120.9	278.0	26.34	321.0	4.91
40/60	120.6	279.1	19.1	320.8	6.13
20/80	120.9	276.6	6.41	320.3	10.5
0/100	—	—	—	310.5	12.58
Heating rate: 20°C/min					
100/0	—	282.3	59.00	—	—
80/20	129.7	278.9	31.09	320.1	0.89
60/40	131.9	279.3	24.67	320.8	1.46
40/60	129.4	278.3	10.97	321.5	5.06
20/80	127.3	279.6	3.19	323.9	7.31
0/100	—	—	—	309.4	11.56

mold seemed to be optimal, because it allows complete crystallization of the pure PPS. However, in the blends, due to a dispersion effect, this time was not enough to crystallize all the PPS fraction. Therefore, when the blends were heated in the DSC cell, the remaining amorphous PPS fraction crystallized. Table II shows these values and the melting entalphies as a function of the heating rate. It is seen that T_{cPPS} remains constant, independently of the PPS fraction; however, it increases with the increase in the heating rate. It can be observed that the melting temperatures of the PPS in the blends are slightly depressed. This can be due to two reasons: Low molecular weight HX4000 molecules, rejected during the HX4000 crystallization, would diffuse into the PPS melt and, during the PPS crystallization, would be entrapped intraspherulitically, producing less perfect PPS crystals, as already observed in Part I of this study[15]; the other reason could be the contribution of less perfect PPS transcrystallites formed on the LCP fibrils surface.[15]

On the other hand, the melting temperatures of the HX4000 in the blends are observed to increase by approximately 10°C, independent of the heating rate. As pointed out by some studies,[23] if the LCP is polydisperse, the higher molecular weight macromolecules will preferentially form the liquid crystalline domains. When blended with PPS, the HX4000 will form an immiscible blend; therefore, as Martuscelli[24] pointed out, "during crystallization at T_c, the processes of phase separation are followed by molecular fractionation and preferential dissolution of smaller and/or more defective molecules of the crystallizable component in the domains more rich in the uncrystallizable polymer B. Thus, the crystallizable matrix will contain more perfect molecules and T_m will increase." In other words, when the HX4000 crystallizes in the presence of PPS, which is immiscible, the HX4000 low molecular weight molecules will be rejected from the crystallizing growth front and will diffuse away. Thus, the HX4000 domains will be formed by molecules of higher molecular weight and more perfectly aligned, which will increase its melting temperatures, as already observed in other blends.[24]

Budgell and Day[12] in their study measured T_{mPPS} and found no variation with the increase of LCP content. Again, the differences between their results and ours could be due to the differences in the blending processes and chemical structure of the LCPs.

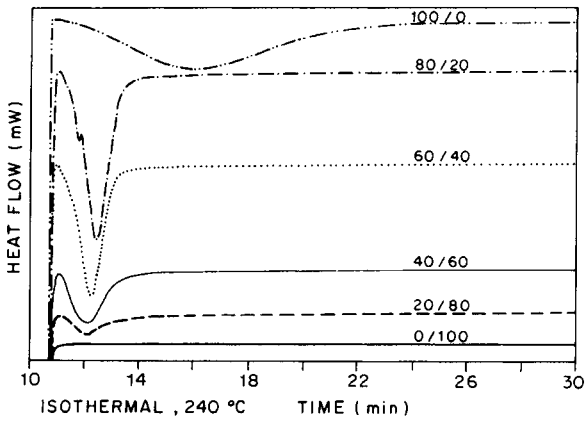

Figure 3 Isothermal crystallization curves of the PPS/HX4000 blends, at 240°C.

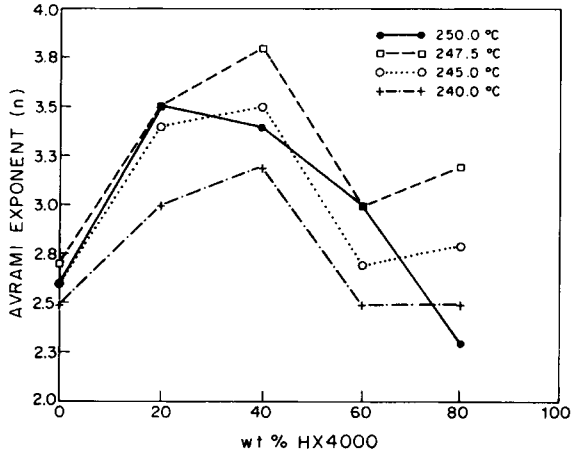

Figure 5 Avrami exponent n as a function of composition, at different crystallization temperatures.

Isothermal Crystallization

The temperature at which the PPS overall crystallization rate is maximum is around 180°C; for the isothermal experiments, temperatures well above 180°C were used, where the overall crystallization rate is controlled mainly by the nucleation step.

Figure 3 shows a typical isothermal crystallization, at 240°C, of the blends. The corresponding Avrami plot [eq. (1)] is shown in Figure 4. Two different regions can be observed: a linear one and a gentle "roll-off." The Avrami equation assumes linearity (primary crystallization); thus, the "roll-off," which can be attributed to secondary crystallization, cannot be analyzed by the Avrami theory.[13] Therefore, from the linear region of this plot, n and k, as a function of temperature, can be calculated. These parameters are shown in Figures 5 and 6, respectively.

It can be observed that, for pure PPS, independently of the crystallization temperatures, $2.7 < n < 2.5$. This value is slightly lower than the ones found in the literature[3,6,12]; however, from both results, expected for PPS is a spherical three-dimensional morphology due to thermal nucleation.[25]

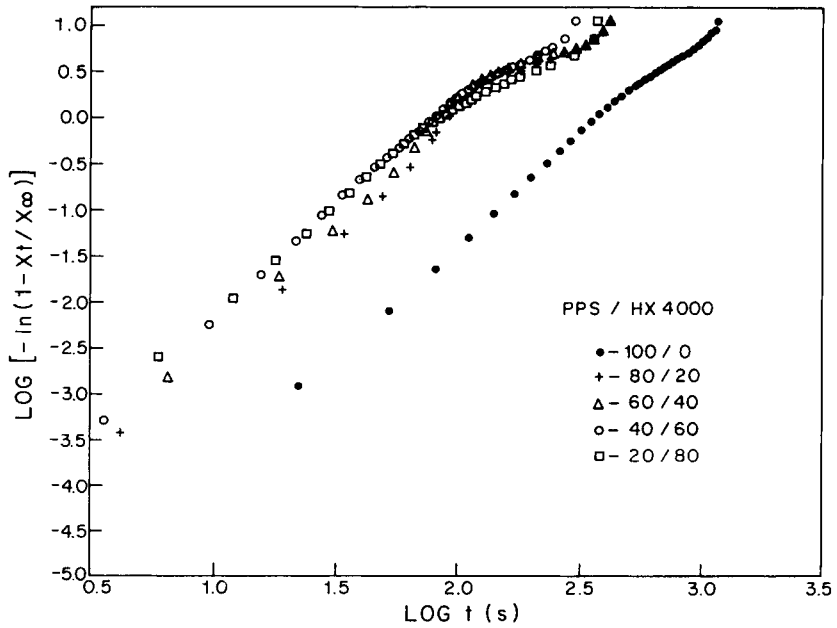

Figure 4 Avrami plots of the PPS/HX4000 blends, at T_c = 240°C.

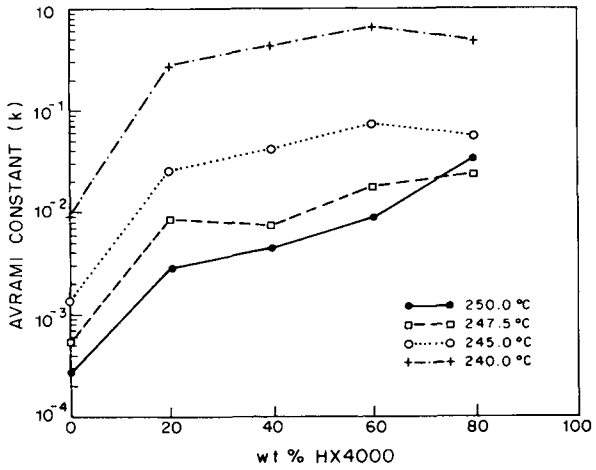

Figure 6 Avrami constant k as a function of composition, at different crystallization temperatures.

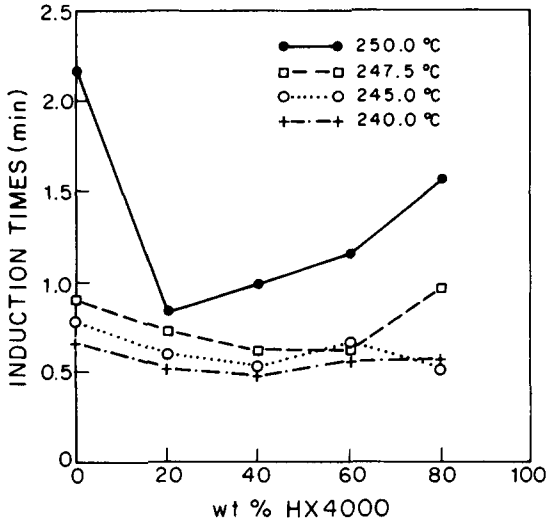

Figure 7 Crystallization induction time t_i of the PPS/HX4000 blends as a function of composition, at different crystallization temperatures.

Regarding the n values as a function of wt % HX4000, two different behaviors can be observed: one at 250°C and the other one at temperatures below 247.5°C. At 250°C, the maximum n value, which would represent higher dimensionality in the morphology, is obtained at a 80/20 composition; afterward, n decreases with the increase of the amount of HX4000. Below 247.5°C, this maximum is observed at the 60/40 compositions; afterward, n decreases up to the 40/60 composition and again increases with the amount of HX4000. In general, up to a concentration of 40 wt % HX4000, the addition of the LCP molecules to the PPS increases the dimensionality of the PPS crystalline morphology, at all compositions and crystallization temperatures. These n values are higher than the ones found by Budgell and Day[12]; they found that the presence of the LCP did not change n. Again, the discrepancies could be due to the differences in melt time and chemical structure of the LCPs. It is known, e.g., that Vectra forms a porous structure when blended with PPS,[18] which can be due to gas liberation from additives in the LCP or chemical reaction between both components. This porous structure was not observed in our blends.

Regarding the k values, it is observed that in the blends the PPS crystallization rate is higher than in the pure state, at all crystallization temperatures and at all compositions; this rate increases with the decrease in crystallization temperature, as expected. Because at those temperatures the nucleation rate is the controlling step, it can be concluded that the increase in the PPS overall crystallization rate in the blends is due to the contribution given by the heterogeneous nucleation of PPS on the HX4000 fibrils.[15]

Other parameters that can be studied from these isothermal scannings are the induction times (time for crystallization to begin), t_i, and the maximum crystallization time (time at which $dQ/dt = 0$, where Q = heat flux), t_{max}. Figure 7 shows t_i as a function of the wt % HX4000. It can be observed that t_i decreases with decrease of the crystallization temperature, as expected. At 250°C, the addition of 20 wt % HX4000 reduces drastically the PPS t_i, but a fur-

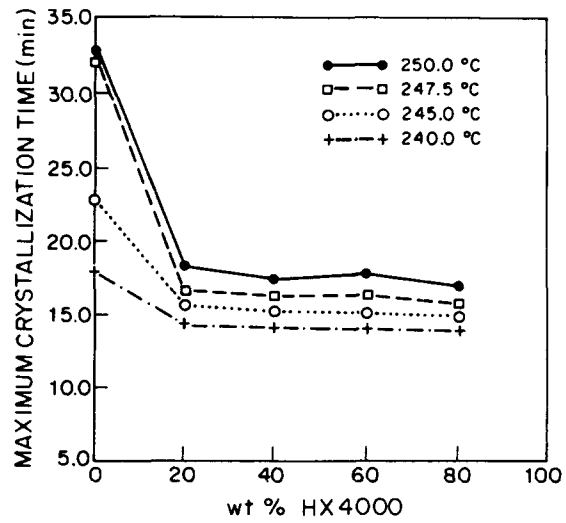

Figure 8 Maximum crystallization time, t_{max}, of the PPS/HX4000 blends as a function of composition, at different crystallization temperatures.

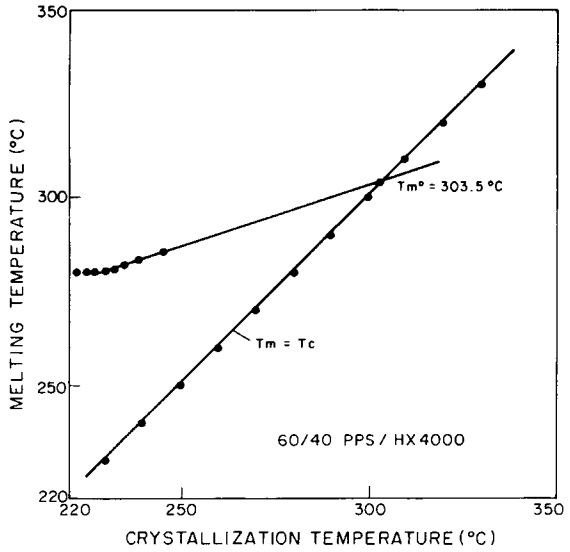

Figure 9 Typical Hoffmann and Weeks plot of a 60/40 PPS/HX4000 blend.

ther increase in the amount of this LCP raises t_i again. Below 247.5°C, there is a tendency for t_i to decrease with increase in the amount of HX4000. Figure 8 shows the t_{max} as a function of wt % HX4000. At all crystallization temperatures, the behavior is similar; whatever the amount of HX4000 added, there is a reduction in the PPS t_{max}, between 44 (at 250°C) and 22% (at 240°C). At a given composition, t_{max} also decreases with the decrease of the temperature, as expected. This data confirms the acceleration of the PPS crystallization by the addition of the HX4000, probably due to heterogeneous nucleation.

Equilibrium Melting Points

Figure 9 shows a typical Hoffmann and Weeks plot of a 60/40 composition. Table III presents the values of T_m^0 for all compositions. As can be seen, T_m^0 did not vary regularly with composition.

Fold Interfacial Free Energy

To calculate σ_e, the following parameters[1] were used: U^* = 1400 cal/mol; C_2 = 30°C; ΔH_m^0 = 80 J/g; b_0 = 5.6 A; σ = 16.9 erg/cm^2; and r = 2. The chosen value of σ = 16.9 erg/cm^2 (Ref. 1) needs further explanation. This value was calculated from the Thomas–Stavely equation,[1] $\sigma = \beta \Delta H_m^0 (A_0)^{1/2}$, where β is a constant depending on the chemical structure of the polymer and A_0 is the cross-sectional area of the chain in the crystal. β is usually equal to 0.1 for polyolefins and 0.24 for some polyesters. Lovinger[1] chose β = 0.3 because the value of σ using β = 0.1 was too low. This criterion was not accurate, but to calculate σ would require further and elaborate experimental work.[2]

Table III Equilibrium Melting Temperature T_m^0 of the PSS/HX4000 Blends

Blend PPS/HX4000	T_m^0 (°C)
100/0	300.9
80/20	299.8
60/40	303.5
40/60	303.7
20/80	301.6

Regarding its constancy, it should be mentioned that in a previous work[13] on blends of PEEK and HX4000 we concluded that neither σ nor σ_e could be considered constants for those particular blends; in fact, the presence of the HX4000 rigid chains would decrease the σ that the PEEK macromolecules would expend on crystallization, resulting in more extended crystals. PEEK and HX4000 were found to have miscibility of their amorphous phases (only one T_g was found) and eq. (4) was applied without constraints. Therefore, we will expect that if the PPS/HX4000 blends are miscible, neither σ nor σ_e would remain constant on blending.

The T_g's values of the PPS/HX4000 blends after annealing were already measured in Ref. 15 and are reproduced in Table IV. Two well-defined T_g's are observed. The T_g of the PPS in the blend does not change with composition. However, the T_g of the LCP has a small decrease with the decrease in the amount of LCP. Therefore, regarding miscibility between PPS and the HX4000 amorphous parts, two

Table IV Glass Transition Temperatures of the PPS/HX4000 Blends[13]; Standard Deviations Are Given in Parentheses

Blends PPS/HX4000	T_g (PPS) (°C)	T_g (HX4000) (°C)
100/0	114.10 (0.32)	—
80/20	114.30 (1.35)	155.56 (0.77)
60/40	115.22 (0.46)	156.36 (0.47)
40/60	115.68 (1.62)	155.70 (2.39)
20/80	115.61 (2.90)	156.60 (3.00)
0/100	—	161.08 (0.85)

Table V σ_e as a Function of Composition, Assuming (a) Immiscibility and (b) Partial Miscibility

Blend PPS/HX4000	σ_e (erg/cm^2) (a)	Correlation Coefficient	σ_e (erg/cm^2) (b)	Correlation Coefficient
100/0	39.80	0.9993	39.80	0.9993
80/20	40.98	0.9991	37.40	0.9983
60/40	44.02	0.9966	39.90	0.9964
40/60	50.42	0.9943	45.10	0.9939
20/80	39.35	0.9679	36.20	0.9892

possibilities can be considered: immiscibility or slight miscibility (partial miscibility).

If we consider that total immiscibility between both components occurs, then eq. (3) can be used to compute σ_e. These values are given in Table V. On the other hand, if we assume partial miscibility, the volume fractions of the PPS in the blend, ϕ_1, need to be calculated; this can be done by using the following equation[26]:

$$\omega_{1,1} = (T_{g_{1,b}} - T_{g_2})/(T_{g_1} - T_{g_2}) \quad (5)$$

where $\omega_{1,1}$ = apparent weight fraction of polymer 1 (PPS) in the polymer 1-rich phase, T_{g_1}, T_{g_2} = T_g's of pure polymers 1 and 2 (HX4000), and $T_{g_{1,b}}$ = observed T_g of polymer 1 in the blends.

The apparent volume fraction of PPS in the PPS-rich phase, $\phi_{1,1}$, can be calculated by dividing $\omega_{1,1}$ by the specific density of polymer 1, ρ_1 = 1.3. These values are given in Table VI; Figure 10 shows a typical plot of α as a function of $1/T\ \Delta T(\phi)\ f$, when partial miscibility is assumed. The σ_e values, assuming partial miscibility, are also given in Table 5.

It can be observed that, when total immiscibility is assumed, σ_e has values between 39.8 (pure PPS) and 50.4 (40/60 blend) erg/cm^2; when partial miscibility is assumed, σ_e vary between 36.2 (20/80 blend) and 45.1 (40/60 blend) erg/cm^2. In other words, the PPS folding works when total immiscibility with the HX4000 is assumed are similar to the folding works when partial miscibility is considered. Also, even without having standard deviations to compare, it can be seen that the variation of σ_e with blend composition is very small. These values are similar to the ones found for other rigid aromatic polymers like PEEK.[13]

Table VI Apparent Weight and Volume Fractions of PPS in the PPS-rich Phase

Blend (PPS/HX4000)	$\omega_{1,1}$	$\phi_{1,1}$
100/0	1	1
80/20	0.9756	0.7501
60/40	0.9695	0.7453
40/60	0.9426	0.7243
20/80	0.9250	0.7169

CONCLUSIONS

Some conclusions can be drawn from this crystallization kinetics analysis:

(a) During the nonisothermal scannings, both components have their crystallization temperatures increased by 10°C; however, the PPS melting temperature is slightly de-

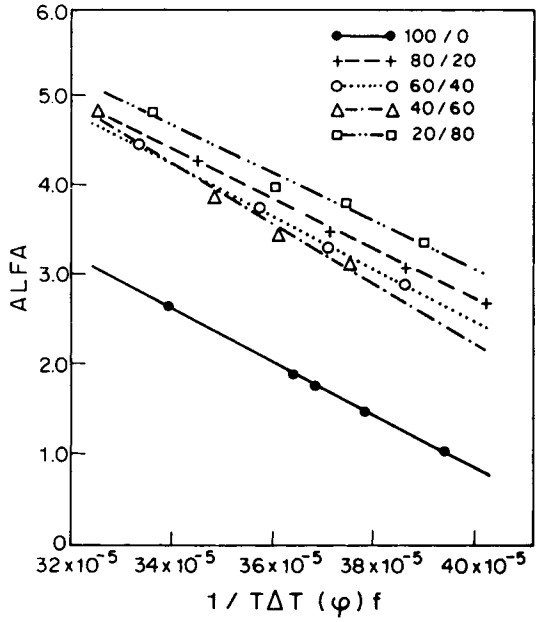

Figure 10 Plot of α as a function of temperature assuming partial miscibility.

creased, while that of the HX4000 is increased by 10°C.

(b) The addition of HX4000 to the PPS increases the dimensionality of the PPS crystalline morphology and increases the PPS overall crystallization rate at all compositions, due to heterogeneous nucleation of the PPS on the HX4000 fibrils surface.

(c) The σ_e of PPS did not vary on blending with the LCP when a σ = 16.9 erg/cm^2 is assumed, contrary to what was observed in a previous work[13] with the same LCP. However, the blends of this last study (PEEK/HX4000) were miscible, while PPS and HX4000 were not; also, it was assumed that the LCP conformation in the melt state was more similar to the lateral surface of the PEEK crystallizing molecule and, therefore, the LCP would affect the value of σ in these blends.

The authors wish to express their gratitude to FAPESP (92/0990-2), CNPq (400770/93-8), and the Volkswagen Foundation (I69693) for their financial support and to Prof. Donald G. Baird for the preparation of the blends.

REFERENCES

1. A. J. Lovinger, D. D. Davis, and F. J. Padden, Jr., *Polymer,* **26,** 1595 (1985).
2. J. D. Hoffmann, G. T. Davis, and J. I. Lauritzen, Jr., *Treatise on Solid State Chemistry,* N. B. Hanray, ed., Plenum, New York, 1976, Vol. 3, p. 497.
3. L. C. Lopez and G. L. Wilkes, *Polymer,* **29,** 106 (1988).
4. J. D. Hoffmann and R. L. Miller, *Macromolecules,* **21,** 3038 (1988).
5. L. C. Lopez and G. L. Wilkes, *Polymer,* **30,** 881 (1989).
6. L. C. Lopez and G. L. Wilkes, *Polymer,* **30,** 147 (1989).
7. V. L. Shingankuli, J. P. Jog, and V. M. Nadkarni, *J. Appl. Polym. Sci.,* **36,** 335 (1988).
8. V. L. Shingankuli, J. P. Jog, and V. M. Nadkarni, *J. Appl. Polym. Sci.,* **51,** 1463 (1994).
9. C. Auer, G. Kalinka, Th. Krause, and G. Hinrichsen, *J. Appl. Polym. Sci.,* **51,** 407 (1994).
10. R. E. S. Bretas, D. Collias, and D. G. Baird, *Polym. Eng. Sci.,* **34,** 1492 (1994).
11. M. T. Heino and J. V. Seppala, *J. Appl. Polym. Sci.,* **44,** 2185 (1992).
12. D. R. Budgell and M. Day, *Polym. Eng. Sci.,* **31,** 17 (1991).
13. B. de Carvalho and R. E. S. Bretas, *J. Appl. Polym. Sci.,* **55,** 233 (1995).
14. L. Minkova, M. Paci, M. Parcella, and P. Magagnini, *Polym. Eng. Sci.,* **32,** 57 (1992).
15. G. Gabellini, M. de Moraes, and R. E. S. Bretas, *J. Appl. Polym. Sci.,* **60,** 21 (1996).
16. R. E. S. Bretas, M. C. B. de Jesus, and G. J. Lunardi, *J. Mater. Sci.,* **27,** 2345 (1992).
17. K. Mai, M. Zhang, H. Zeng, and S. Qi, *J. Appl. Polym. Sci.,* **51,** 57 (1994).
18. A. Valenza, F. P. La Mantia, L. I. Minkova, S. de Petris, M. Paci, and P. L. Magagnini, *J. Appl. Polym. Sci.,* **52,** 1653 (1994).
19. P. Cebe and S. Hong, *Polymer,* **27,** 1183 (1986).
20. G. B. A. Lim and D. R. Lloyd, *Polym. Eng. Sci.,* **33,** 513 (1993).
21. G. C. Alfonso, V. Chiappa, J. Liu, and E. R. Sadiku, *Eur. Polym. J.,* **27,** 795 (1991).
22. B. S. Hsiao and B. B. Sauer, *J. Polym. Sci. Part B Polym. Phys.,* **31,** 901 (1993).
23. J. I. Kroschwitz, Ed., *High Performance Polymers and Composites—Liquid Crystalline Polymers,* Wiley, New York, 1991.
24. E. Martuscelli, *Polym. Eng. Sci.,* **24,** 563 (1984).
25. B. Wunderlich, *Macromolecular Physics,* Academic Press, New York, 1976, Vol. 2.
26. W. N. Kim and C. M. Burns, *Macromolecules,* **20,** 1876 (1987).

Received October 10, 1995
Accepted March 30, 1996